PROCEEDINGS OF SCIENCE

Electron acceleration and advection model for the high energy emission from the large scale jet of AGNs

Amal A. Rahman,[a,*] **Sunder Sahayanathan**[b,c] **and P. A Subha**[a]

[a] *Farook College, Calicut University, Kerala - 673632, India*

[b] *Bhabha Atomic Research Centre, Mumbai - 400085, India*

[c] *Homi Bhabha National Institute, Mumbai - 400094, India*

E-mail: amalar.amal@gmail.com

The detection of hard X-ray emission from the kilo-parsec scale jet of active galactic nuclei cannot be interpreted as the synchrotron emission mechanism from the electron distribution responsible for the radio/optical emission. The X-ray emission when interpreted as the inverse-Compton scattering of cosmic microwave background photons (IC/CMB process), the Compton spectral component will peak at GeV energy. The non-detection of significant gamma-ray flux from these large-scale jets by *Fermi* disfavoured this model, particularly at low redshifts. Alternately, synchrotron emission from a different electron population is suggested. However, the X-ray emissions from the jet of AGN at high redshift are usually interpreted as IC/CMB process, due to the increase in cosmic microwave background (CMB) photon density. But, recent *Fermi* γ-ray flux upper limit estimates on jet emission from the high redshift source J1510+5702 questions the validity of the IC/CMB model. In this work, we consider a model where the multi-spectral component (MSC) emissions from the large-scale jets of AGN is explained using accelerated and advected electron distributions [1]. The synchrotron emission from these two electron distribution is capable of interpreting the MSC jet emission from the jet of J1510+5702.

High Energy Phenomena in Relativistic Outflows VIII (HEPROVIII)
23-26 October, 2023
Paris, France

*Speaker

© Copyright owned by the author(s) under the terms of the Creative Commons Attribution-NonCommercial-NoDerivatives 4.0 International License (CC BY-NC-ND 4.0).

PoS(HEPROVIII)017

1. Introduction

The jets from active galactic nuclei (AGN) can reach distances of kpc to Mpc and contain bright emission regions known as knots [2]. These knots, resolved in radio and optical wavebands were observed in X-ray as well with the advent of *Chandra*. The radio-to-optical emission from the knots is generally attributed to the synchrotron process [3, 4], whereas the X-ray emission process is modelled either as inverse Compton scattering of soft target photons or synchrotron emission. This is based on the value of optical-to-X-ray spectral index (α_{ox}) in comparison to radio-to-optical spectral index (α_{ro}) [5]. For $\alpha_{ox} > \alpha_{ro}$, the X-ray emission is explained as the high energy extent of synchrotron emission responsible for radio-optical emission. On the other hand, when $\alpha_{ox} < \alpha_{ro}$, it is attributed to inverse Compton emission or synchrotron emission from a different/second electron population [3, 6–8].

Synchrotron Self Compton (inverse Compton process associated with the synchrotron photons themselves) is disfavored as a possible mechanism of X-ray emission since it demands a magnetic field that deviates largely from the equipartition condition [2, 4]. X-ray knots when modeled using the IC/CMB emission mechanism suggest the spectral component to peaks at γ-ray energies and predicts that the jets of nearby AGN can be detectable by the *Fermi* space telescope operating at γ-ray energies [9]. However, *Fermi* γ-ray observation of 3C 273 during 2008-2013 resulted only in flux upper limits, contradicting the predicted detectable flux [10]. A similar result was obtained for many other sources [11, 12], which disfavours the IC/CMB model and advocates the presence of a second electron population which is responsible for the observed X-ray emission from the knots.

The IC/CMB interpretation of X-ray emission for misaligned AGN jets is still preferred at high redshifts, due to the increase in CMB energy density ($U_{\rm CMB} \propto (1+z)^4$) [13]. Hence, the study of the large-scale jet at high redshifts can be used as a tool to validate this [14–16]. The resolved X-ray jet of PKS J1421-0643 (at $z = 3.69$) and PSO J030947.49+271757.31 ($z = 6.1$) were modelled with the IC/CMB interpretation [17, 18]. Recently, Breiding et al. [19] examined the IC/CMB interpretation for 45 extra-galactic X-ray jets. They found that the IC/CMB model is questioned in 27 Multi-Spectral Component (MSC) X-ray jets due to over-prediction for the observed MeV-to-GeV γ-ray flux. Their sample had three jets located at higher redshifts ($z > 3.5$). Out of these three sources, the IC/CMB interpretation of X-ray emission from J1510+5702 and J1421-0643 is ruled out considering the estimated γ-ray flux upper limits.

In our previous study [1], we explore the possible origin of the second electron population to interpret the MSC emission from the large-scale jet of AGN. We particularly considered a scenario where the high-energy electrons from the sites of particle acceleration advect into the jet medium, resulting in the formation of two spatially separated electron populations. In this study, we apply this model to a high redshift source J1510+5702 to explain the MSC jet emission. This is the highest redshift source for which the IC/CMB interpretation of X-ray emission is ruled out through gamma-ray flux upper limit estimates.

PoS(HEPROVIII)017

2. The two-population model

The model considered in our study is explained in detail in [1]. According to this model, synchrotron emission from a a broken power-law electron distribution of particles confined to the acceleration region interprets the high energy (X-ray) emission. The accelerated electrons leave this region and advect out losing energy in the process. This results in a particle distribution with an excess of low-energy particles. The synchrotron emission associated with this particle distribution explains the lower energy emission (radio) in the jet.

3. J1510+5702

Siemiginowska et al. [20] and Yuan et al. and [21] first reported the kilo-parsec scale X-ray emission from the quasar J1510+5702, which is located at a redshift of 4.3. The X-ray emission feature, located a few arcsecs away from the quasar core, was previously interpreted as IC/CMB radiation. This source appeared in the Fermi/LAT 4FGL 8-year point source catalog and this data was used to estimate the flux upper limits in gamma rays [19]. The study finds that IC/CMB model is ruled out for interpreting the X-ray emission considering the gamma-ray flux upper limit estimates.

4. Results and Discussion

We applied the electron acceleration and advection model described above to reproduce the MSC jet emission from the kilo-parsec scale jet of J1510+5702. The synchrotron emission from the broken power-law distribution confined within region R < R0 successfully interprets the X-ray flux. Whereas, the advected electron distribution from the region R > R0 constitutes the low energy electron distribution and the synchrotron emission from this population reproduces the observed radio fluxes. The superposition of the radiated spectra from the two zones gives a composite spectrum and can explain the optical observations as well. In Fig. 1 (left), the MSC observations of the jet of J1510+5702 along with model curves are plotted. On the right, we show the observed radio–optical–X-ray fluxes from the knot A for 3C 273 [1] for comparison. The model fit parameters are tabulated in Table. 1.

The IC/CMB model predicts that the radio and X-ray spectral indices match because of an identical electron distribution responsible for emission at these energy bands. However, the X-ray spectral index of the jet in J1510+5702 is harder than the radio. Hence, the IC/CMB spectrum does not align with the observed X-ray spectral index of the jet (see Fig A8 [19]). This suggests the second population of electrons as the possible origin of X-ray emission. The model considered in our study assumes the dominant electron distributions responsible for radio and X-ray emission to be different. This can result in different spectral indices in radio and X-ray energies.

PoS(HEPROVIII)017

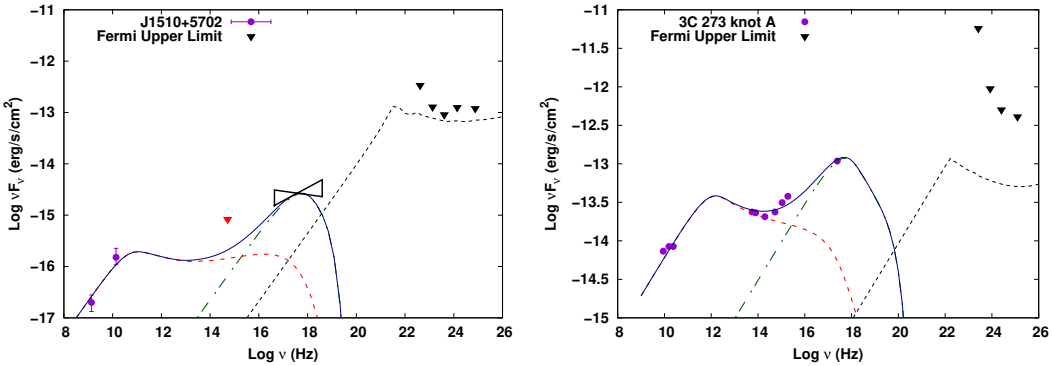

Figure 1: Left figure shows the observed SED of the jet of J1510+5702 along with model curves. The purple solid circle, inverted red triangle and butterfly diagram correspond to radio, optical upper limit and X-ray flux values. Green dot-dash line represents the synchrotron emission from accelerated electron population, red dashed line represents synchrotron emission from advected electron population and blue solid line represent total synchrotron emission (accelerated+advected electron population). The black dashed line corresponds to IC/CMB spectrum and *Fermi* upper limits are denoted by black inverted triangles. The figure in right represent the observed SEDs of the knots A of 3C 273 along with the model curves.

Knot	R_0	R_{size}	$B_{in}(10^{-5}G)$	ω	$\gamma_b(10^7)$	v_{ad}	p	q	Γ
J1510+5702 Jet	0.17	5.0	0.8	1.14	27.7	1.0	1.68	4.0	1.02
3C 273 Knot A	0.12	2.9	1.5	2.08	7.5	2.0	2.0	4.0	1.3

Table 1: Fit parameters of radio-optical-X-ray spectrum. R_0 and R_{size} are the size of inner region and the size of the knot in kpc units; $\omega = \frac{B_{\rm in}}{B_{\rm out}}$ where $B_{\rm in}$ and $B_{\rm out}$ represent the magnetic field strength at $R < R_0$ and $R > R_0$ respectively. The quantities γ_b, v_{ad}, p, q and Γ represent the break energy, advection velocity, power law indices of broken power law distribution of particles and bulk Lorentz factor respectively.

The IC/CMB model demands significant jet speed to explain the X-ray emission which in turn predicts one-sided jets due to relativistic de-beaming of the counter jet. However, the detection of the counter jet in Pictor A disfavors the IC/CMB origin of the X-ray emission [22]. Our model considers a slow jet at kilo-parsec scales assuminging that the jet loses most of its kinetic energy in the initial parsec scale region. Moreover, no significant positional changes in the emission regions are noticed for the jets at kpc scale. The model also considers two regions (acceleration and advection) with different but comparable magnetic fields. The magnetic field in the acceleration region can be slightly larger because the acceleration process can amplify the magnetic field in the region. Moreover, any mechanism that can significantly modify the magnetic field in the acceleration (shock) and advection regions are still unknown.

The redshift dependence of X-ray to radio luminosity of blazars was studied by many [23–26]. The IC/CMB contribution towards this effect was also examined [27, 28]. A

PoS(HEPROVIII)017

study done on 17 highly radio loud quasars at $z > 4$ showed 3 times enhancement in X-ray emission when compared to similar sources at lower redshifts [29]. One of the prominent radiation fields present at the large-scale jet of AGN is CMB radiation. The increase in CMB energy density with redshift should be evident in the IC/CMB spectrum if it is the emission governing the X-ray emission in large-scale jets. However, the gamma-ray upper limits rule out the IC/CMB predictions. The model proposed in the work has the potential to interpret the MSC jet emission from the lower redshift sources (3C 273) as well as the high redshift source for which the IC/CMB model is ruled out. Dedicated *Chandra* observations along with infra-red and optical observations for more high redshift sources can provide clues on the proposed model and in validating the IC/CMB model for the X-ray emission from large-scale jets.

PoS(HEPROVIII)017

References

[1] A.A. Rahman, S. Sahayanathan and P.A. Subha, *Advection of accelerated electrons in radio/X-ray knots of AGN jets*, **515** (2022) 1410 [2206.07324].

[2] D.E. Harris and H. Krawczynski, *X-Ray Emission from Extragalactic Jets*, **44** (2006) 463 [astro-ph/0607228].

[3] J. Kataoka and Ł. Stawarz, *X-Ray Emission Properties of Large-Scale Jets, Hot Spots, and Lobes in Active Galactic Nuclei*, **622** (2005) 797 [astro-ph/0411042].

[4] J. Zhang, J.M. Bai, L. Chen and E. Liang, *X-Ray Radiation Mechanisms and Beaming Effect of Hot Spots and Knots in Active Galactic Nuclear Jets*, **710** (2010) 1017 [0912.2470].

[5] S. Jester, D.E. Harris, H.L. Marshall and K. Meisenheimer, *New Chandra Observations of the Jet in 3C 273. I. Softer X-Ray than Radio Spectra and the X-Ray Emission Mechanism*, **648** (2006) 900 [astro-ph/0605529].

[6] A. Atoyan and C.D. Dermer, *Synchrotron versus Compton Interpretations for Extended X-Ray Jets*, **613** (2004) 151 [astro-ph/0402647].

[7] D.E. Harris, A.E. Mossman and R.C. Walker, *The X-Ray Jet of 3C 120: Evidence for a Nonstandard Synchrotron Spectrum*, **615** (2004) 161 [astro-ph/0407354].

[8] Y. Uchiyama, C.M. Urry, C.C. Cheung, S. Jester, J. Van Duyne, P. Coppi et al., *Shedding New Light on the 3C 273 Jet with the Spitzer Space Telescope*, **648** (2006) 910 [astro-ph/0605530].

[9] M. Georganopoulos, E.S. Perlman, D. Kazanas and J. McEnery, *Quasar X-Ray Jets: Gamma-Ray Diagnostics of the Synchrotron and Inverse Compton Hypotheses: The Case of 3C 273*, **653** (2006) L5 [astro-ph/0610847].

[10] E.T. Meyer and M. Georganopoulos, *Fermi Rules Out the Inverse Compton/CMB Model for the Large-scale Jet X-Ray Emission of 3C 273*, **780** (2014) L27 [1307.8421].

[11] E.T. Meyer, M. Georganopoulos, W.B. Sparks, L. Godfrey, J.E.J. Lovell and E. Perlman, *Ruling out IC/CMB X-rays in PKS 0637-752 and the Implications for TeV Emission from Large-scale Quasar Jets*, **805** (2015) 154 [1504.00577].

[12] P. Breiding, E.T. Meyer, M. Georganopoulos, M.E. Keenan, N.S. DeNigris and J. Hewitt, *Fermi Non-detections of Four X-Ray Jet Sources and Implications for the IC/CMB Mechanism*, **849** (2017) 95 [1710.04250].

PoS(HEPROVIII)017

[13] D.E. Harris and H. Krawczynski, *X-Ray Emission Processes in Radio Jets*, **565** (2002) 244 [astro-ph/0109523].

[14] B. Snios, D.A. Schwartz, A. Siemiginowska, M. Sobolewska, M. Birkinshaw, C.C. Cheung et al., *Discovery of Candidate X-Ray Jets in High-redshift Quasars*, **914** (2021) 130 [2102.12609].

[15] Y. Zhang, T. An, S. Frey, K.É. Gabányi and Y. Sotnikova, *Radio Jet Proper-motion Analysis of Nine Distant Quasars above Redshift 3.5*, **937** (2022) 19 [2209.10760].

[16] B. Snios, D.A. Schwartz, A. Siemiginowska, M. Sobolewska, M. Birkinshaw, C.C. Cheung et al., *X-Ray Jets in the High-redshift Quasars J1405+0415 and J1610+1811*, **934** (2022) 107.

[17] D.M. Worrall, M. Birkinshaw, H.L. Marshall, D.A. Schwartz, A. Siemiginowska and J.F.C. Wardle, *Inverse-Compton scattering in the resolved jet of the high-redshift quasar PKS J1421-0643*, **497** (2020) 988 [2007.03536].

[18] L. Ighina, A. Moretti, F. Tavecchio, A. Caccianiga, S. Belladitta, D. Dallacasa et al., *Direct observation of an extended X-ray jet at $z = 6.1$*, **659** (2022) A93 [2111.08632].

[19] P. Breiding, E.T. Meyer, M. Georganopoulos, K. Reddy, K.E. Kollmann and A. Roychowdhury, *A multiwavelength study of multiple spectral component jets in AGN: testing the IC/CMB model for the large-scale-jet X-ray emission*, **518** (2023) 3222 [2210.13104].

[20] A. Siemiginowska, R.K. Smith, T.L. Aldcroft, D.A. Schwartz, F. Paerels and A.O. Petric, *An X-Ray Jet Discovered by Chandra in the z=4.3 Radio-selected Quasar GB 1508+5714*, **598** (2003) L15 [astro-ph/0310241].

[21] W. Yuan, A.C. Fabian, A. Celotti and P.G. Jonker, *Extended X-ray emission in the high-redshift quasar GB 1508+5714 at z= 4.3*, **346** (2003) L7 [astro-ph/0309318].

[22] M.J. Hardcastle, E. Lenc, M. Birkinshaw, J.H. Croston, J.L. Goodger, H.L. Marshall et al., *Deep Chandra observations of Pictor A*, **455** (2016) 3526 [1510.08392].

[23] K. Toda, Y. Fukazawa and Y. Inoue, *Cosmological Evolution of Flat-spectrum Radio Quasars Based on the Swift/BAT 105 Month Catalog and Their Contribution to the Cosmic MeV Gamma-Ray Background Radiation*, **896** (2020) 172 [2005.02648].

[24] X. Shen, P.F. Hopkins, C.-A. Faucher-Giguère, D.M. Alexander, G.T. Richards, N.P. Ross et al., *The bolometric quasar luminosity function at $z = 0$-7*, **495** (2020) 3252 [2001.02696].

PoS(HEPROVIII)017

[25] M. Ajello, L. Costamante, R.M. Sambruna, N. Gehrels, J. Chiang, A. Rau et al., *The Evolution of Swift/BAT Blazars and the Origin of the MeV Background*, **699** (2009) 603 [0905.0472].

[26] P.F. Hopkins, G.T. Richards and L. Hernquist, *An Observational Determination of the Bolometric Quasar Luminosity Function*, **654** (2007) 731 [astro-ph/0605678].

[27] S.F. Zhu, W.N. Brandt, J. Wu, G.P. Garmire and B.P. Miller, *Investigating the X-ray enhancements of highly radio-loud quasars at $z > 4$*, **482** (2019) 2016 [1810.06572].

[28] E. Hodges-Kluck, E. Gallo, G. Ghisellini, F. Haardt, J. Wu and B. Ciardi, *Proof of CMB-driven X-ray brightening of high-z radio galaxies*, **505** (2021) 1543 [2105.03467].

[29] J. Wu, W.N. Brandt, B.P. Miller, G.P. Garmire, D.P. Schneider and C. Vignali, *An X-Ray and Multiwavelength Survey of Highly Radio-loud Quasars at $z > 4$: Jet-linked Emission in the Brightest Radio Beacons of the Early Universe*, **763** (2013) 109 [1301.0012].

PoS(HEPROVIII)017